

## Supplementary Materials

### ***In vitro* biological and *in silico* screening of the novel iron(III) complexes for DNA-targeted antitumor drug component**

Serap Nigdelioglu Dolanbay<sup>1</sup>, Zehra Kübra Yilmaz<sup>1</sup>, Büşra Kaya<sup>2\*</sup>, Belma Aslim<sup>1</sup>, Bahri Ülküseven<sup>2</sup>

<sup>1</sup>Gazi University, Faculty of Science, Department of Biology, 06500 Ankara, Turkey

<sup>2</sup>Department of Chemistry, Engineering Faculty, Istanbul University-Cerrahpasa, 34320, Avcilar, Istanbul, Turkey

**Table S1.** SMILES notations of complexes from Cheminfo software.

Complexes	SMILES notations*
Fe1	c1ccc2c(c1)O[Fe]13(OC(=C(C(c4cccc4)OC)C(=[N]1N=C(SC)[N]3=C2)C)C)Cl
Fe2	c1(ccc2c(c1)O[Fe]13(OC(=C(C(c4cccc4)OC)C(=[N]1N=C(SC)[N]3=C2)C)C)Cl)OC

\* SMILES notations used in Molinspiration and PASS online software.

**Table S2.** Selected supercoiled pBR322 DNA cleavage data in the presence of varying concentrations of complex **Fe1** in Fig. 7.

Lane no.	Reaction conditions	Form I (%)	Form II (%)
0	DNA	87.5	12.5
1	DNA+ Fe1 (500 µM)	83.3	16.7
2	DNA+ Fe1 (750 µM)	71.1	28.9
3	DNA+ Fe1 (1000 µM)	80.7	19.3
4	DNA+ Fe1 (1500 µM)	66.9	33.1
5	DNA+ Fe1 (2500 µM)	22.5	77.5

**Table S3.** Selected supercoiled pBR322 DNA cleavage data in the presence of varying concentrations of complex **Fe2** in Fig. 7.

Lane no.	Reaction conditions	Form I (%)	Form II (%)
0	DNA	90.2	9.8
1	DNA+ Fe2 (500 µM)	86.4	13.6
2	DNA+ Fe2 (750 µM)	84.3	15.7
3	DNA+ Fe2 (1000 µM)	81.5	18.5
4	DNA+ Fe2 (1500 µM)	83.9	16.1
5	DNA+ Fe2 (2500 µM)	75.4	24.6

**Table S4.** The optimized geometrical parameters of Fe(III) complexes 1 and 2 in the ground state at the B3LYP/LANL2DZ level, together with the published crystal data<sup>1</sup>.

Bond length (Å)	Calculated		Experimental
Complexes	Fe1	Fe2	Similar structure <sup>1</sup>
Fe1-O1	1.872	1.872	1.897(2)
Fe1-O3	1.877	1.876	1.907(2)
Fe1-N1	1.893	1.894	2.067(3)
Fe1-N3	1.941	1.942	2.076(3)
Fe1-Cl1	2.290	2.293	2.2146(11)
Bond angle (deg)			
O1-Fe1-O3	91.6	91.6	92.51(10)
O1-Fe1-N1	89.3	89.4	87.07(10)
O3-Fe1-N1	167.0	167.0	144.71(11)
O1-Fe1-N3	158.4	158.3	147.74(11)
O3-Fe1-N3	91.2	91.1	87.47(11)
N1-Fe1-N3	83.2	83.2	74.99(11)
O1-Fe1-Cl1	102.4	102.4	108.50(8)
O3-Fe1-Cl1	100.3	100.5	108.66(9)
N1-Fe1-Cl1	92.2	92.0	104.86(8)
N3-Fe1-Cl1	98.7	98.8	102.00(9)

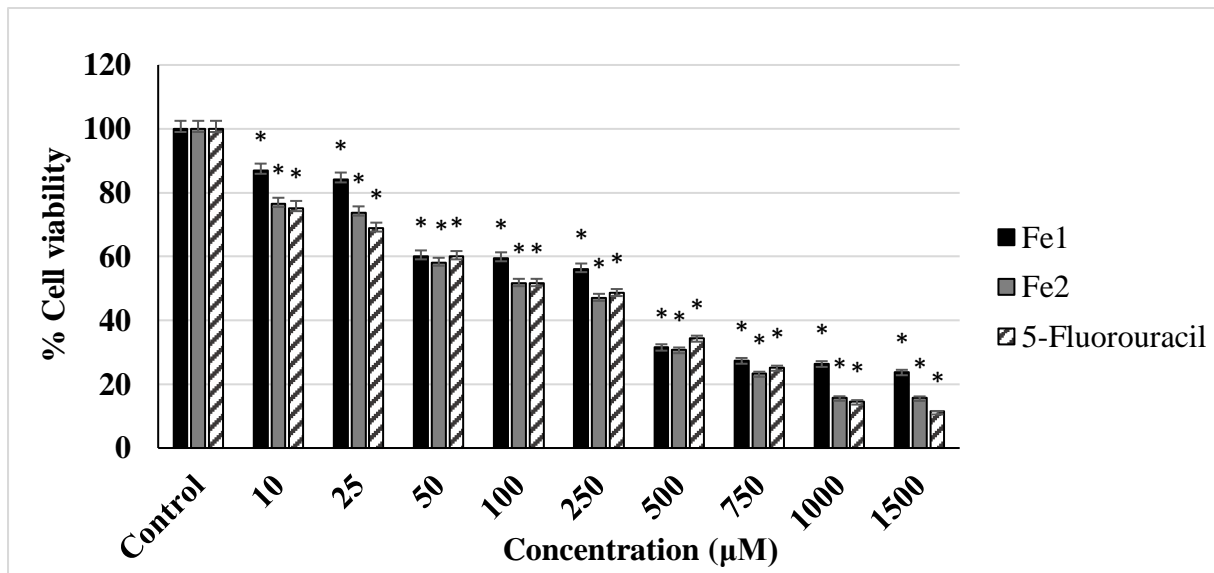


**Figure S1a.** The effects of complexes **Fe1**, **Fe2** and 5-Fluorouracil on viability of HT-29 cell line for 24 h. Results are represented as mean of three replicates  $\pm$  standard deviation. \* $p < 0.05$  compared to control.

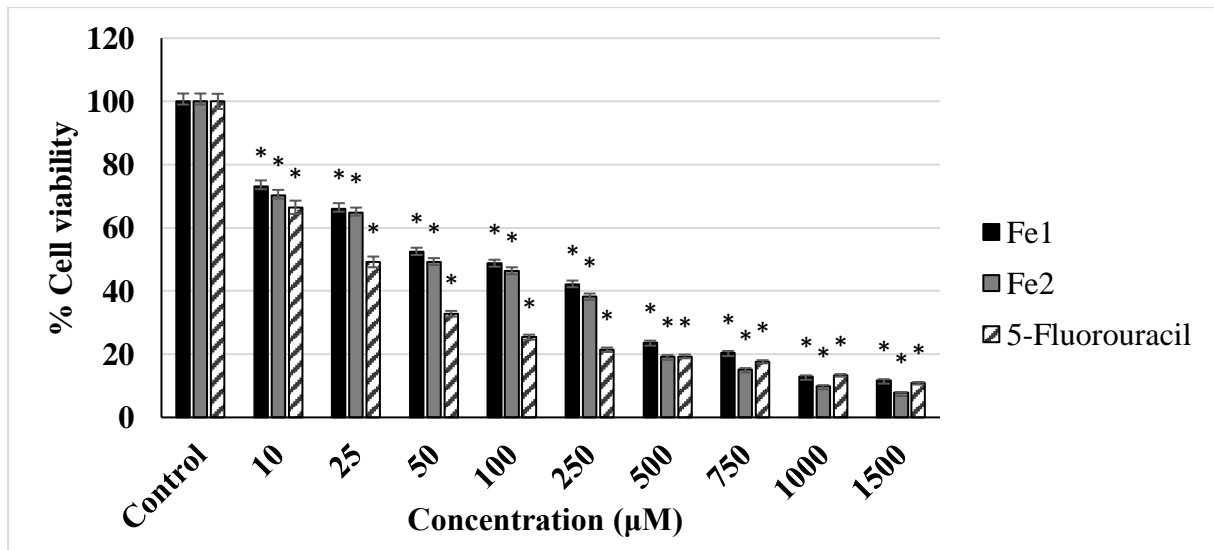


**Figure S1b.** The effects of complexes **Fe1**, **Fe2** and 5-Fluorouracil on viability of HT-29 cell line for 48 h. Results are represented as mean of three replicates  $\pm$  standard deviation. \* $p < 0.05$  compared to control.

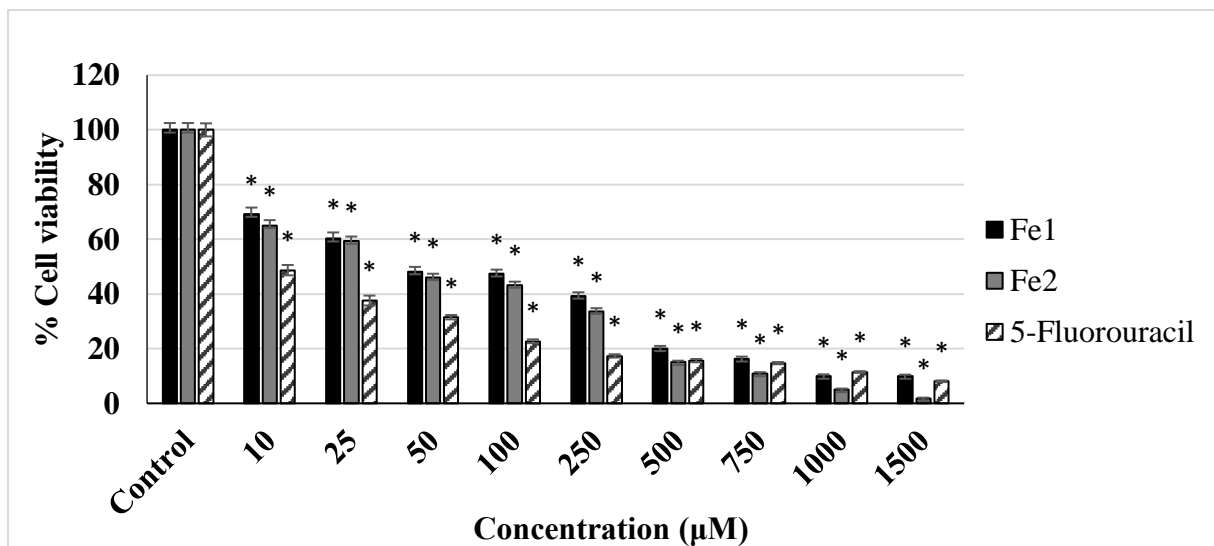


**Figure S1c.** The effects of complexes **Fe1**, **Fe2** and 5-Fluorouracil on viability of (a) HT-29 cell line for 72 h. Results are represented as mean of three replicates  $\pm$  standard deviation. \* $p < 0.05$  compared to control.

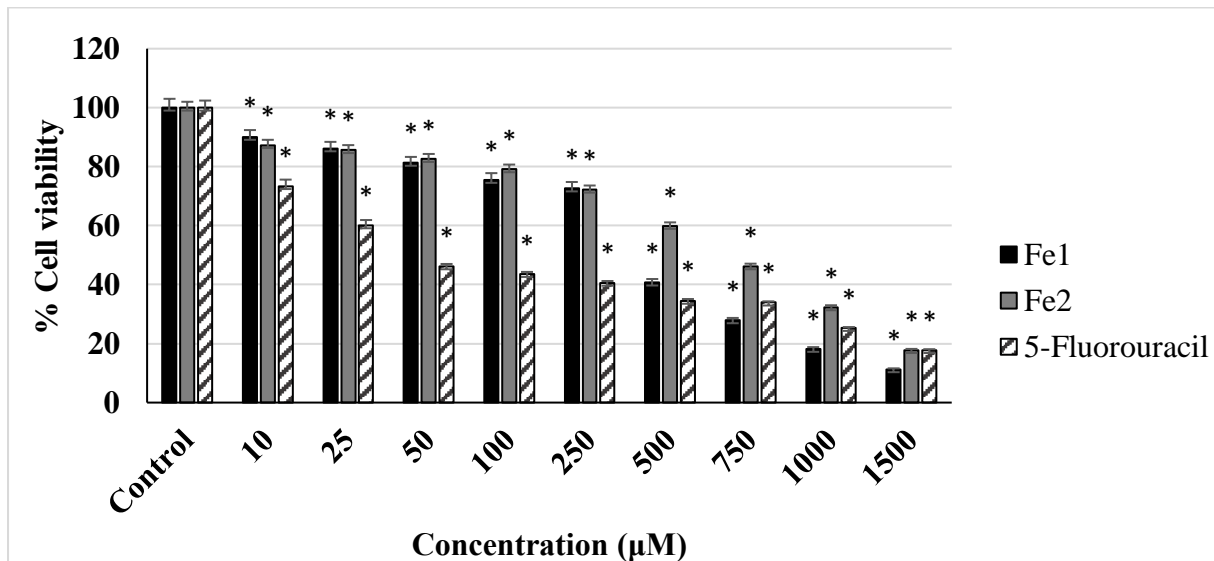


**Figure S2a.** The effects of complexes **Fe1**, **Fe2** and 5-Fluorouracil on viability of HeLa cell line for 24 h. Results are represented as mean of three replicates  $\pm$  standard deviation. \* $p < 0.05$  compared to control.

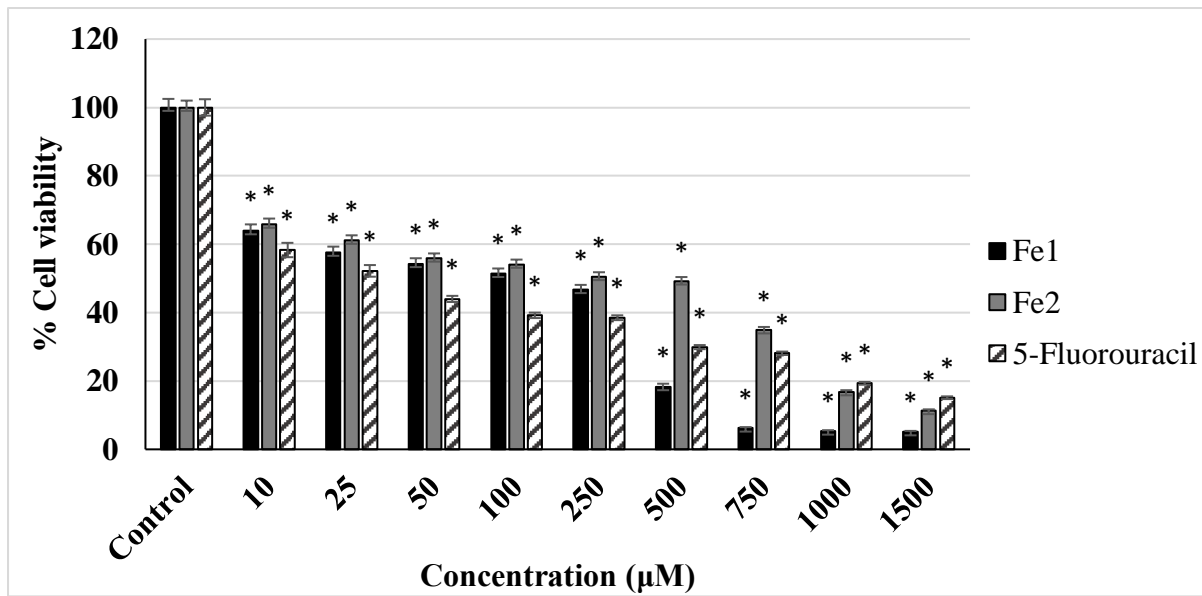


**Figure S2b.** The effects of complexes **Fe1**, **Fe2** and 5-Fluorouracil on viability of HeLa cell line for 48 h. Results are represented as mean of three replicates  $\pm$  standard deviation. \* $p < 0.05$  compared to control.

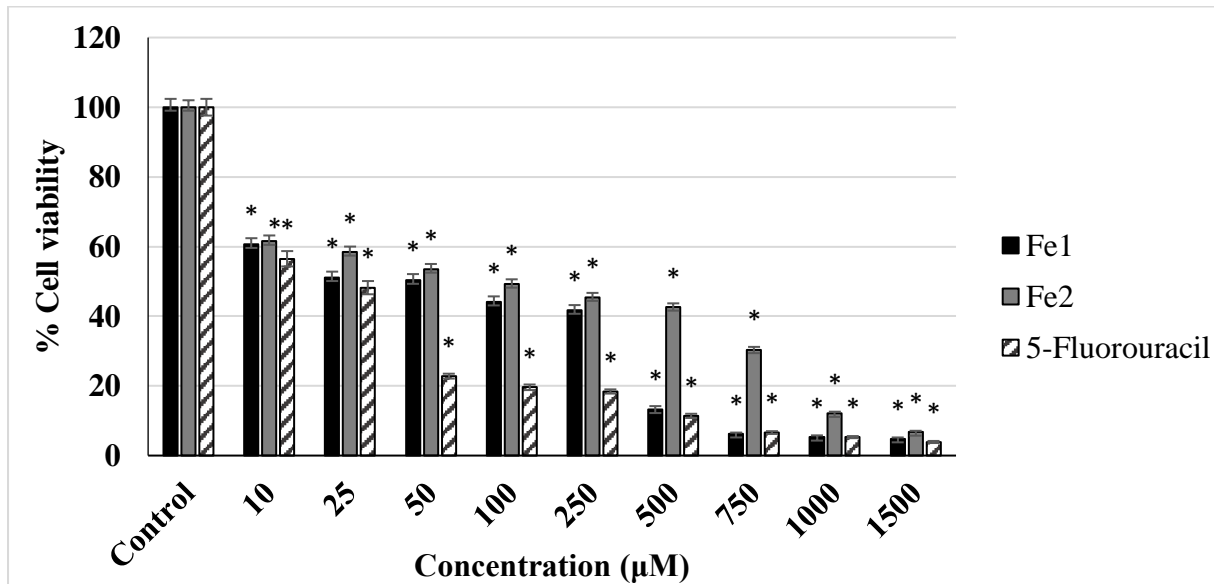


**Figure S2c.** The effects of complexes **Fe1**, **Fe2** and 5-Fluorouracil on viability of HeLa cell line for 72 h. Results are represented as mean of three replicates  $\pm$  standard deviation. \* $p < 0.05$  compared to control.

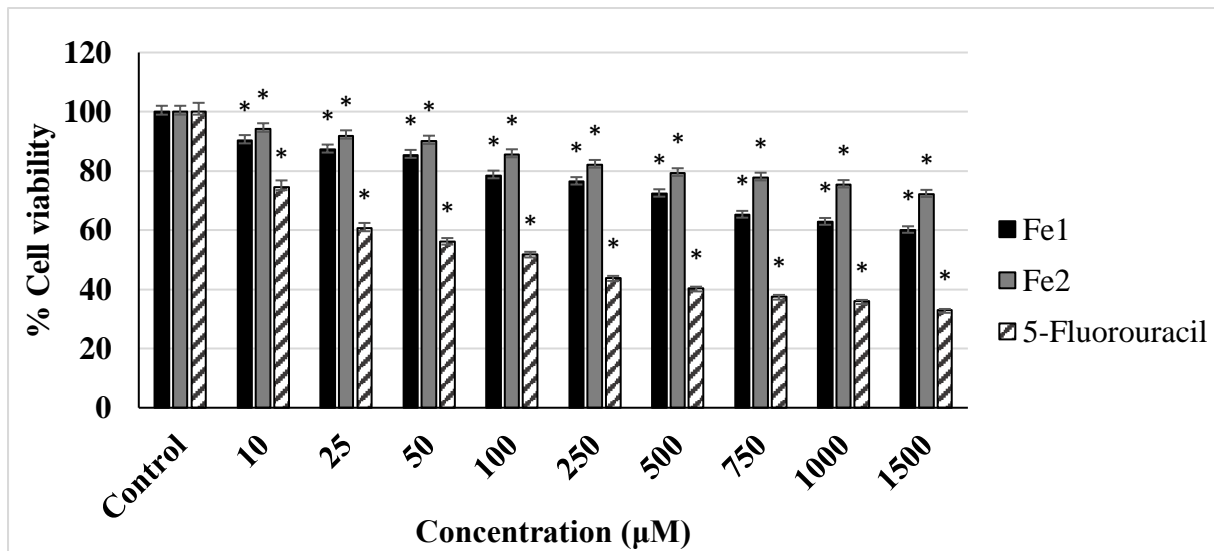


**Figure S3a.** The effects of complexes **Fe1**, **Fe2** and 5-Fluorouracil on viability of L929 cell line for 24 h. Results are represented as mean of three replicates  $\pm$  standard deviation. \* $p < 0.05$  compared to control.

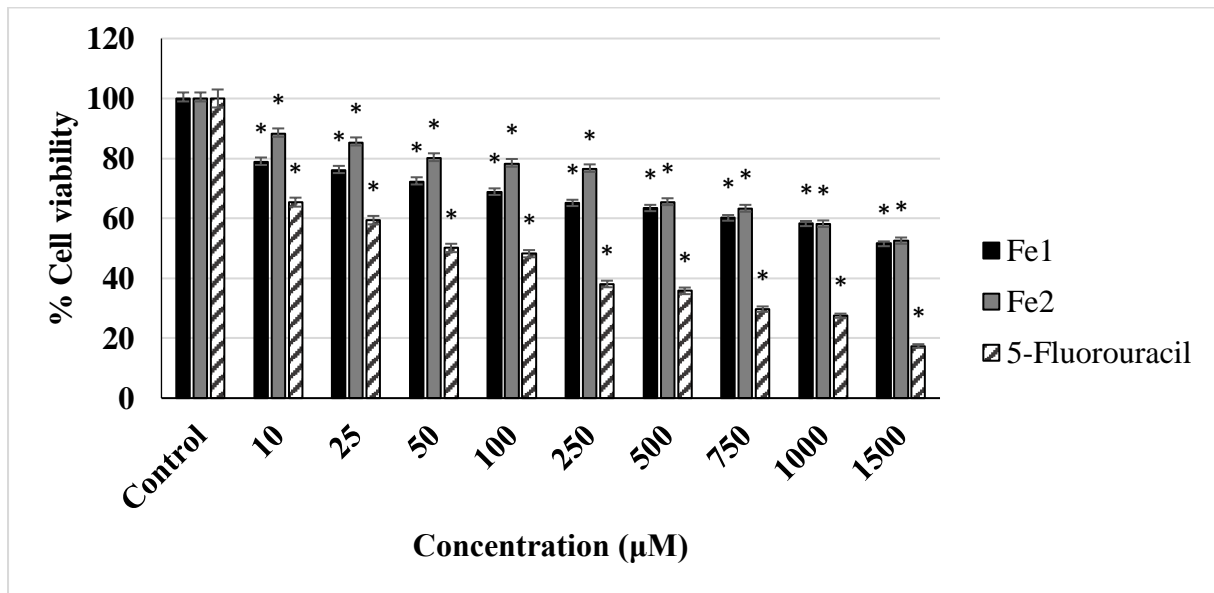


**Figure S3b.** The effects of complexes **Fe1**, **Fe2** and 5-Fluorouracil on viability of L929 cell line for 48 h. Results are represented as mean of three replicates  $\pm$  standard deviation. \* $p < 0.05$  compared to control.

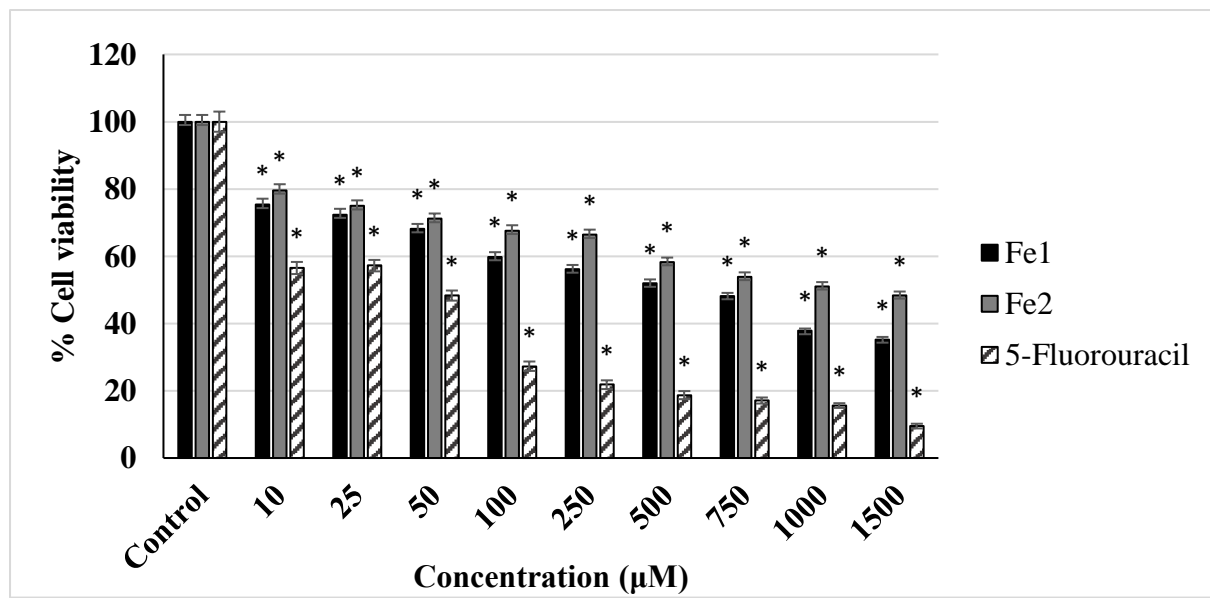


**Figure S3c.** The effects of complexes **Fe1**, **Fe2** and 5-Fluorouracil on viability of L929 cell line for 72 h. Results are represented as mean of three replicates  $\pm$  standard deviation. \* $p < 0.05$  compared to control.

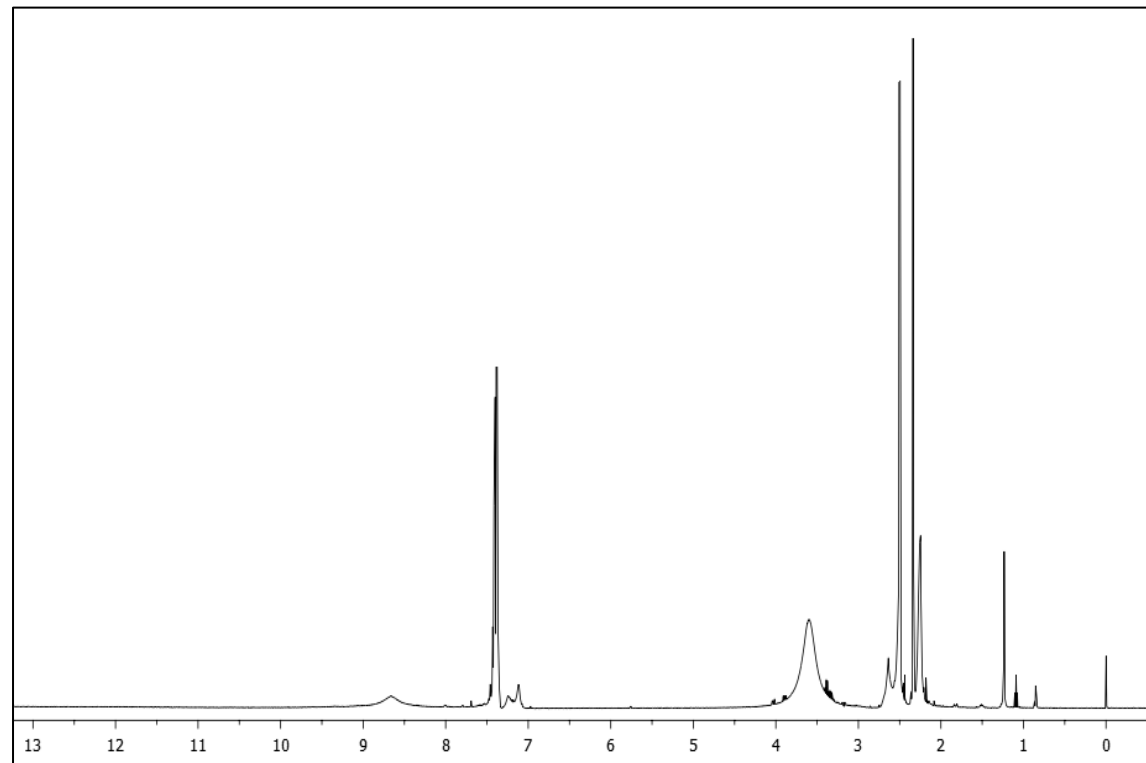


**Figure S4.**  $^1\text{H}$  NMR spectrum of 3-benzylidene-2,4-pentanedione-S-methylthiocarbazone hydrogen iodide in  $\text{DMSO-d}_6$ .

Fe1 #68-76 RT: 1.89-2.09 AV: 9 NL: 3.27E8  
T: + c ESI ms [ 50.00-2000.00 ]

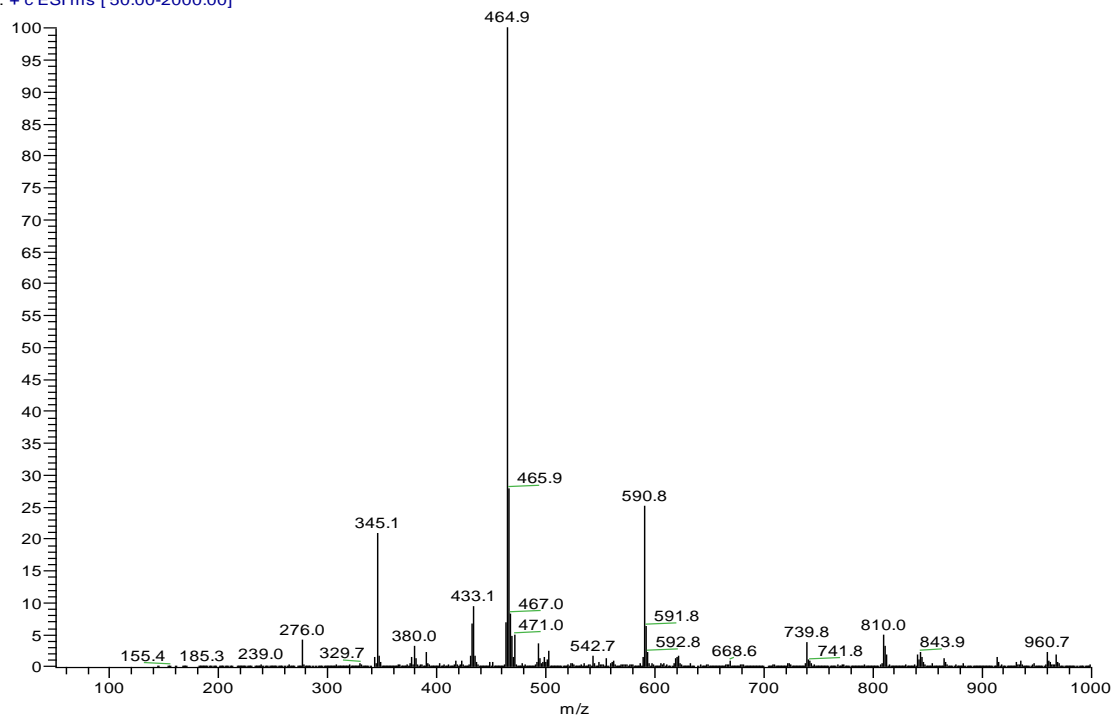


**Figure S5.** ESI-MS of Fe1 in  $\text{CHCl}_3$ .

Fe2 #110-134 RT: 2.99-3.60 AV: 25 NL: 2.39E8  
T: + c ESI ms [ 50.00-2000.00 ]

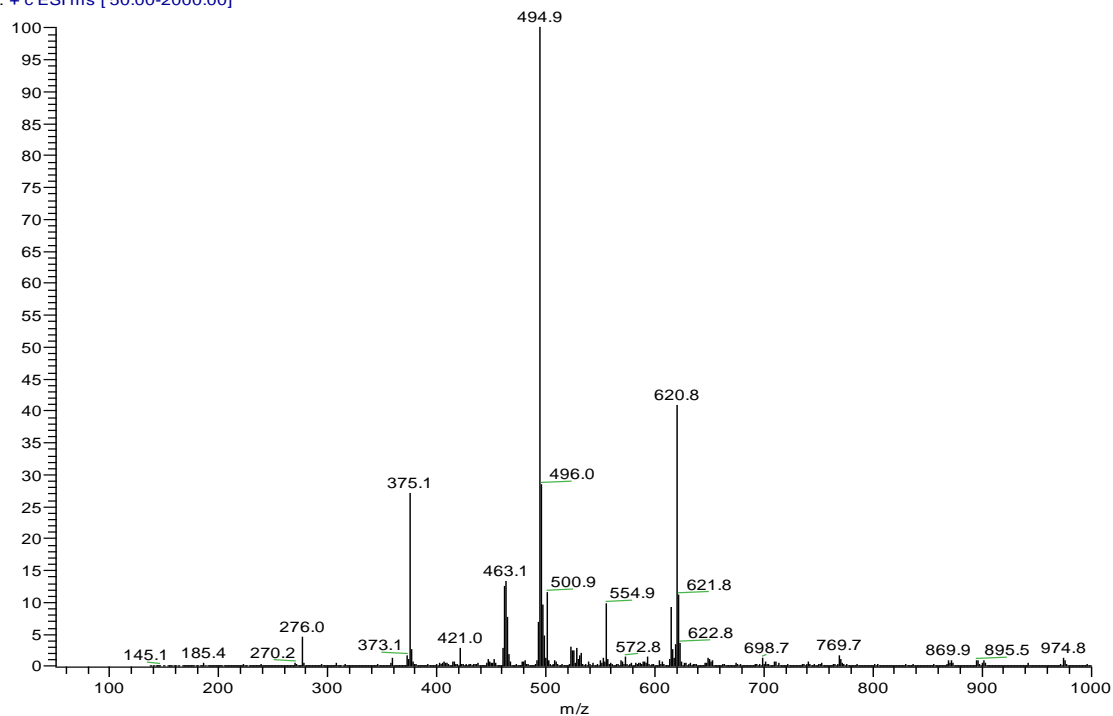


**Figure S6.** ESI-MS of Fe2 in  $\text{CHCl}_3$ .

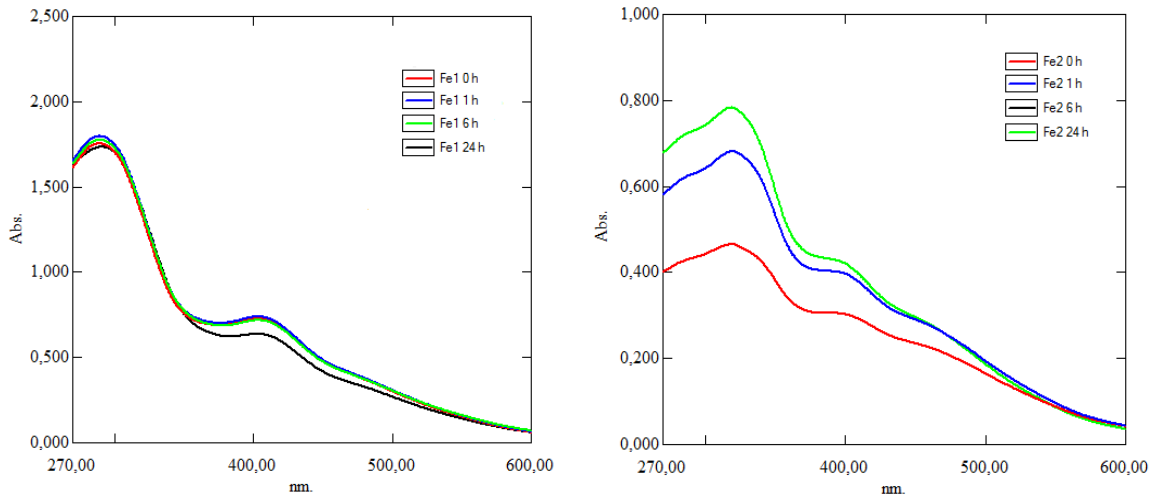


**Figure S7.** UV-Visible spectra of **Fe1** and **Fe2** in 1% DMSO-water mixture.

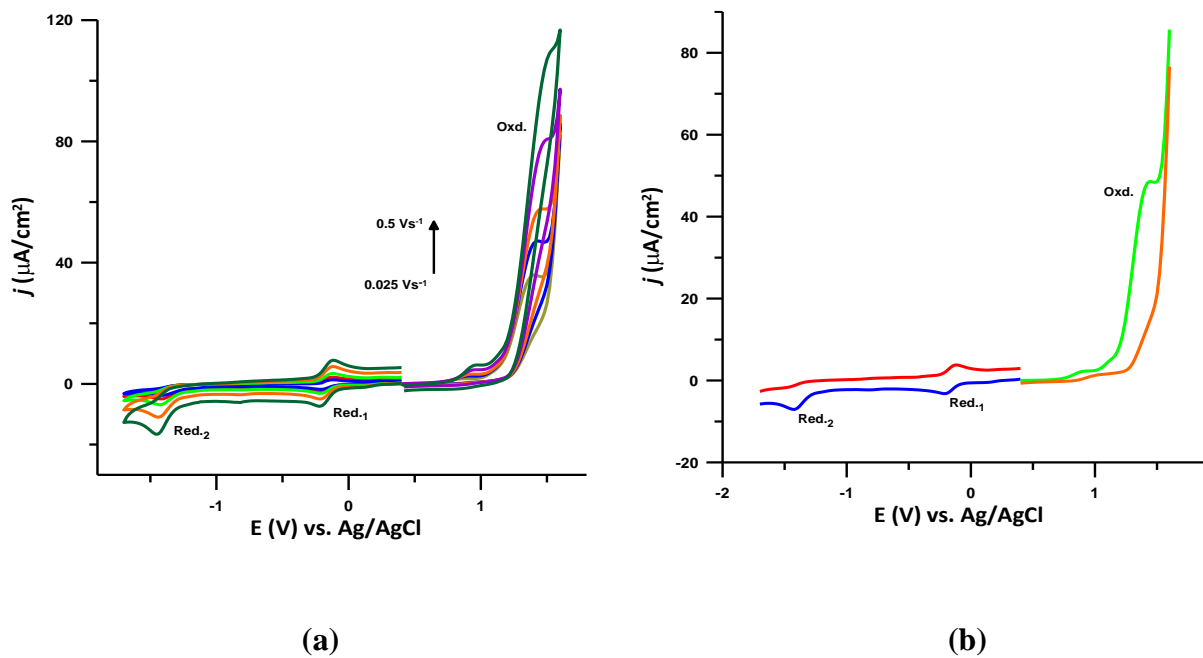


**Figure S8.** CVs of **Fe1** ( $1.0 \times 10^{-3}$  M) at different scan rates (0.025, 0.05, 0.1, 0.25, 0.5 Vs<sup>-1</sup>) (a) and LSVs at a scan rate of 0.1 Vs<sup>-1</sup> in 0.1 M TBAP/DMSO solution on GC working electrode (b).

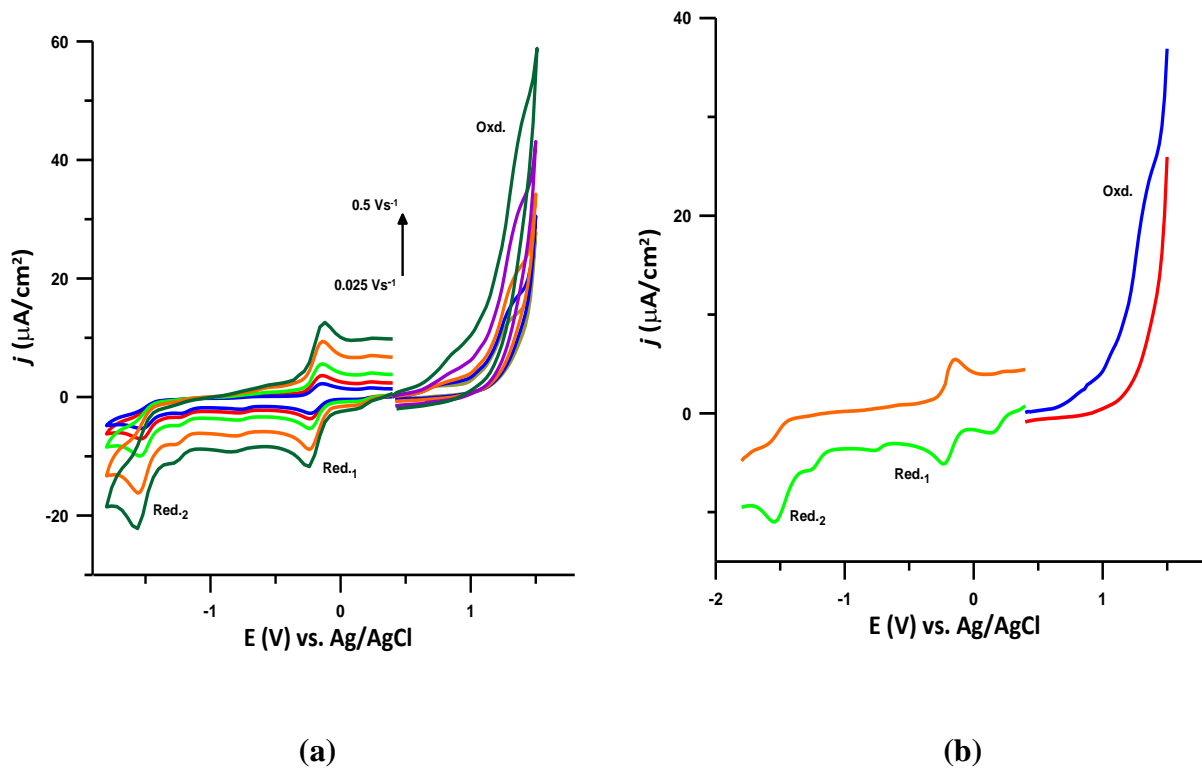


**Figure S9.** CVs of **Fe2** ( $1.0 \times 10^{-3}\text{M}$ ) at different scan rates ( $0.025, 0.05, 0.1, 0.25, 0.5 \text{ Vs}^{-1}$ ) (a) and LSVs at a scan rate of  $0.1 \text{ Vs}^{-1}$  in  $0.1 \text{ M}$  TBAP/DMSO solution on GC working electrode (b).

## References

1. B. A. Arslan, B. Kaya, O. Şahin, S. Baday, C. C. Saylan and B. Ülküseven, *J. Mol. Struct.*, 2021, **1246**, 131166.